SURFACE CODE QUANTUM ERROR CORRECTION
INCORPORATING ACCURATE ERROR PROPAGATION

AUSTIN G. FOWLER,   DAVID S. WANG,   LLOYD C. L. HOLLENBERG

Centre for Quantum Computer Technology, University of Melbourne
VIC 3010, Australia

The surface code is a powerful quantum error correcting code that can be defined on a 2-D square lattice of qubits with only nearest neighbor interactions. Syndrome and data qubits form a checkerboard pattern. Information about errors is obtained by repeatedly measuring each syndrome qubit after appropriate interaction with its four nearest neighbor data qubits. Changes in the measurement value indicate the presence of chains of errors in space and time. The standard method of determining operations likely to return the code to its error-free state is to use the minimum weight matching algorithm to connect pairs of measurement changes with chains of corrections such that the minimum total number of corrections is used. Prior work has not taken into account the propagation of errors in space and time by the two-qubit interactions. We show that taking this into account leads to a quadratic improvement of the logical error rate.

Communicated by: S Braunstein & G Milburn

1   Introduction

The idea of manipulating quantum systems to perform computation was first proposed by Feynman in 1982 [1]. Serious interest in making this vision a reality followed the invention of Shor's factoring algorithm in 1994 [2]. Initial concerns that unfeasible physical control was required were tempered by the invention of quantum error correction (QEC) in 1995 [3] and proof of the threshold theorem in 1996 [4, 5]. The threshold theorem showed that arbitrarily large quantum computations can be performed arbitrarily reliably provided the error rates of the various components in the quantum computer are all below some fixed threshold error rate p_{th}.

Early work [6] put the value of p_{th} at approximately 10^{-6}. The ability to interact pairs of qubits separated by arbitrarily large distances was also demanded. The current record highest p_{th} of approximately 3% is shared by two quantum computing schemes [7, 8]. Both of these schemes, however, still require the ability to interact pairs of qubits separated by arbitrarily large distances. This is a major barrier to implementation. Studies of the performance of such error correction techniques when they are restricted to 1-D, quasi-1-D and 2-D lattices of qubits with only nearest neighbor interactions [9, 10, 11, 12, 13, 14] have found that the threshold error rate drops to the 10^{-5} level or below.

Topological approaches to quantum error correction [15, 16, 17, 18, 19, 20, 21, 22, 23, 24, 25, 26, 27, 28, 29, 30, 31, 32, 33, 34, 35] can be implemented optimally using only nearest neighbor interactions. Kitaev's surface code [15], which makes use of a 2-D square lattice of qubits with nearest neighbor interactions, possesses the highest threshold error rate of the known topological schemes at approximately 0.75% [18, 30, 33]. This is not far below the record threshold error rate and above some existing experimental error rates [36, 37]. In recent years, a number of quantum computer designs based on this form of error correction have been devised [38, 39, 40, 41, 42, 43] and an experimental demonstration using linear optics has been performed [44]. Many technologies are being developed that are in principle capable of implementing a 2-D lattice of qubits with nearest neighbor interactions, including ion traps [45, 46, 47, 48, 49], neutral atom chips [50, 51], optical lattices [52, 53], superconductors [36, 54] quantum dots [55], donors in silicon [56] and electrons on liquid helium [57].

A number of open problems remain concerning the best way to perform the classical processing associated with surface code QEC. In this paper, we address a major failing of prior approaches [30, 33, 29], which did not take into account the propagation of errors as a result of the two-qubit interactions required to detect errors. We show that, for a given lattice size, carefully taking into account error propagation results in a quadratic improvement of the logical error rate.

The discussion is organized as follows. In Section 2, the surface code is briefly reviewed. Section 3 discusses the standard surface code QEC procedure, its limitations, and numerical results explicitly demonstrating these limitations. Section 4 describes our modification to the standard procedure, its advantages, and numerical results explicitly demonstrating these advantages. Section 5 concludes with a summary of our results.

2   The surface code

In this Section, we briefly describe the surface code, focusing primarily on its stabilizers and the quantum circuits required to measure them. A full description of surface code quantum computing can be found in [30].

A stabilizer of a state $|\Psi\rangle$ is an operator S such that $S|\Psi\rangle = |\Psi\rangle$. Any error E that anti-commutes with S can be readily detected since $SE|\Psi\rangle = -ES|\Psi\rangle = -E|\Psi\rangle$. A generic circuit capable of determining the sign of a stabilizer is shown in Fig. 1a. Surface code stabilizers have the form $XXXX$, XXX, $ZZZZ$ or ZZZ, as shown for the specific case in Fig. 2a. Circuits capable of measuring such stabilizers are shown in Figs. 1b-c. An appropriate sequence of two-qubit gates to use when measuring all stabilizers across the lattice simultaneously is shown in Fig. 2b.

The lattice of Fig. 2a is capable of protecting a single qubit of information from errors. This protected qubit is called a logical qubit and can be read out in the logical X/Z basis by measuring all data qubits in the physical X/Z basis. After error correction, which we shall describe in the next Section, the logical measurement result is equal to the product of X/Z measurement results along paths connecting boundaries as shown in Fig. 2c. The distance d of the code is equal to the shortest of these paths. Fig. 2a is an example of a distance $d = 4$ code.
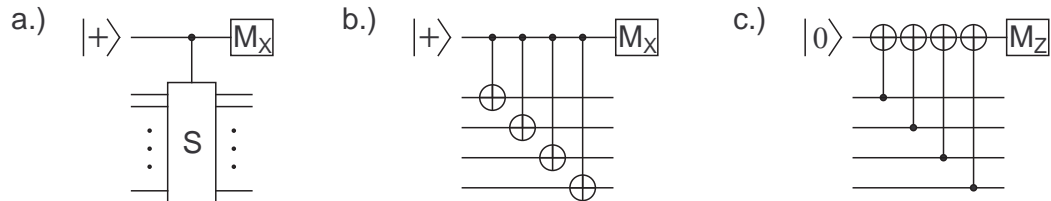
Fig. 1. a.) General circuit determining the sign of a stabilizer S. b.) Circuit determining the sign of a stabilizer $XXXX$. c.) Circuit determining the sign of a stabilizer $ZZZZ$.
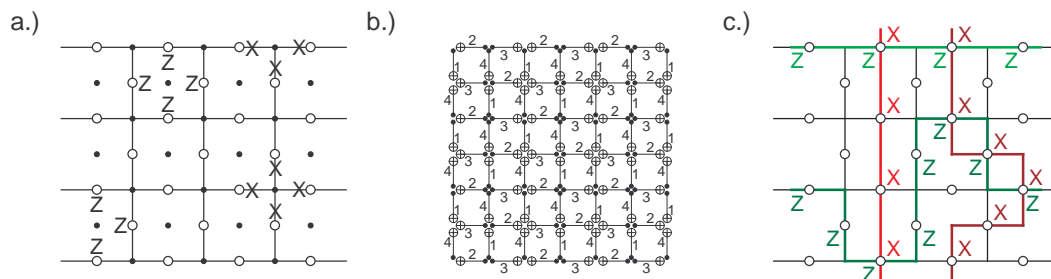
Fig. 2. a.) 2-D lattice of data (open circles) and syndrome (dots) qubits along with examples of the data qubit stabilizers. b.) Sequence of CNOTs permitting simultaneous measurement of all stabilizers. The numbers indicate the relative gate order. c.) Examples of logical operators.

3   Standard surface code QEC

Repeatedly executing the gate sequence shown in Fig. 2b, along with syndrome qubit initialization and measurement, generates data points in space and time where the measurement values change. These are called syndrome changes. Fig. 3a shows an example. The standard method of surface code QEC effectively only considers errors occurring on data qubits at the same time as the syndrome qubits are being measured and errors on the syndrome qubits just before they measured. Such errors are not propagated by the two-qubit gates and have been studied in detail in [16]. A single data qubit error results in two syndrome changes adjacent in space. A single syndrome qubit error results in two syndrome changes adjacent in time. The separation s of two syndrome changes occurring at space-time locations (i_1, j_1, t_1), (i_2, j_2, t_2) is defined to be $s = |i_1 - i_2| + |j_1 - j_2| + |t_1 - t_2|$. In other words, the standard approach assumes that an error chain containing at least s errors must occur to produce the observed syndrome changes. The minimum weight matching algorithm [58, 59] is used to process the list of space-time locations, matching pairs of locations such that the total of all separations is a minimum. An example of the input to and output of this algorithm is shown in Fig. 3. The algorithm itself is highly complex, and will not be discussed here. A good introductory explanation of the algorithm can be found in [60], along with links to the current fastest publicly available library function. The construction of faster implementations of this algorithm is an active field of research.

We use the standard error model in which the error rates of initialization, measurement, memory and two-qubit gates are all set to equal p_g. In detail, initialization to $|0\rangle/|+\rangle$ fails with probability p_g resulting in initialization to $|1\rangle/|-\rangle$ respectively. Memory (identity gate) is
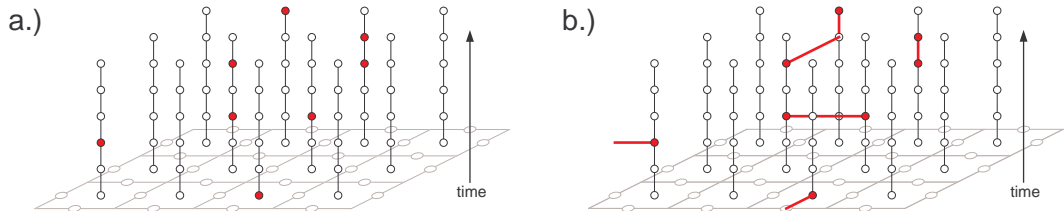
Fig. 3. a.) Locations in space and time, indicated by red dots, where and when the reported syndrome is different from that in the previous time step. Note that this is not a three-dimensional physical structure, just a three-dimensional classical data structure. b.) Optimal matching highly likely to lead to a significant reduction of the number of errors if bit-flips are applied to the spacelike edges.

followed by one of the gates X, Y, Z, each with probability $p_g/3$. Measurement (destructive) reports the wrong eigenstate with probability p_g. Two-qubit gates are followed by one of the 15 nontrivial tensor products of I, X, Y, Z, each with probability $p_g/15$.

The performance of error correction with the standard measure of separation is shown in Fig. 4. Fig. 4 shows the number of rounds of syndrome measurement that can be performed, on average, before a logical error occurs for a range of lattice sizes d and gate error rates p_g. The simulation method is described in detail in [30]. With the exception of the lowest error rate data point of each curve, each data point represents the average of at least 5000 simulation runs. The lowest error rate data points represent the average of at least 500 runs. Lattices are of the form shown in Fig. 2a, meaning each curve represents the average number of rounds of error correction before a single logical qubit protected by the surface code is corrupted. A distance d code should be able to reliably correct $\lfloor (d-1)/2 \rfloor$ errors, implying the logical qubit lifetime should be proportional to $1/p_g^{\lfloor (d+1)/2 \rfloor}$ for low p_g. It can be seen from Fig. 4 that something is seriously wrong. At low p_g, a distance $d = 3$ lattice has a logical error rate proportional to p_g, meaning it offers no genuine error correction ability. Both $d = 5$ and $d = 7$ are only capable of reliably correcting a single error.

The reason the error correction performs suboptimally at low error rates is illustrated in Fig. 5. A single error occurring halfway through syndrome measurement can cause a pair of syndrome changes separated by two units of space and one of time. A chain of such errors as shown in Fig. 6 will be matched as shown in dashed lines, resulting in a logical error. A $d \times d$ lattice can thus only cope with $\lfloor (d-1)/4 \rfloor$ errors in the worst case using this error correction method.

4   Improved surface code QEC

A $d \times d$ lattice should be able to cope with $\lfloor (d-1)/2 \rfloor$ errors in the worst case. We achieve this by modifying the way in which the separation is calculated between a pair of syndrome changes.

Let us consider a slightly more general syndrome measurement procedure than that shown in Fig. 2b. Let us assume that some of the two-qubit interactions are significantly slower than others. Some syndrome measurements may be performed more frequently than others. We permit the order of interaction to vary dynamically to enable syndrome measurements to be performed as frequently as possible. We imposed the necessary condition that it must be
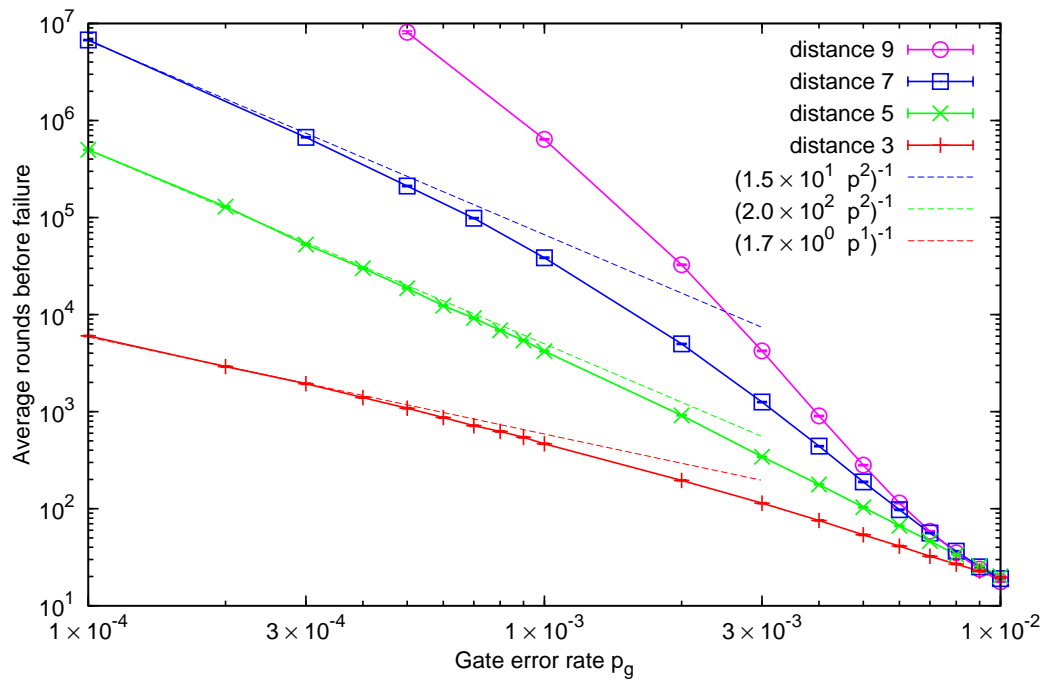
Fig. 4. Average number of rounds of error correction before the logical qubit is corrupted as a function of the physical gate error rate p_g and code distance d when the standard measure of separation s of syndrome changes is used. Asymptotic curves have been included.
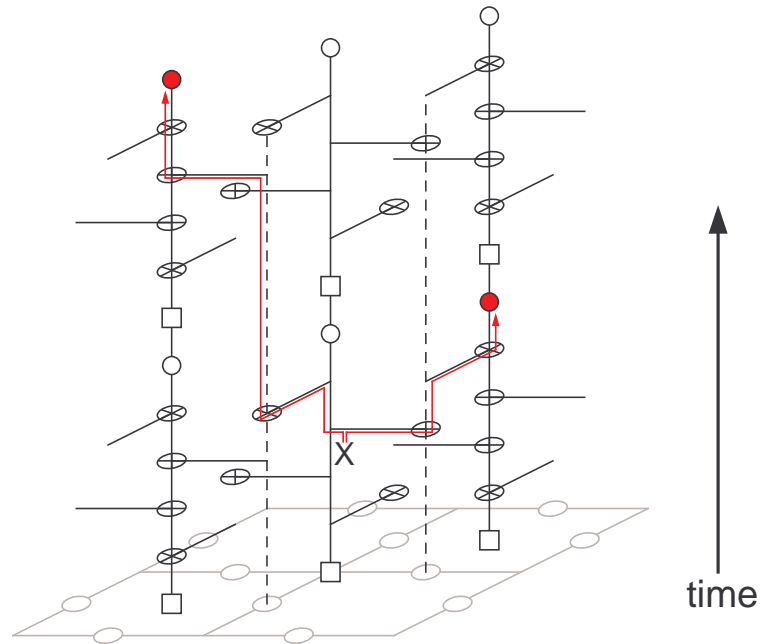
Fig. 5. Errors on syndrome qubits can propagate to two locations separated by two units of space and one unit of time.
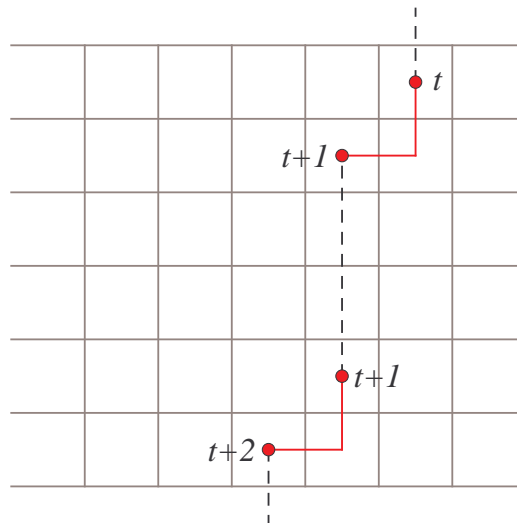
Fig. 6. Two errors of the form shown in Fig. 5 can cause a distance $d = 7$ code to fail when simple syndrome change separations are used. The dashed lines indicate five operators that will be suggested as appropriate corrections but will in fact form a logical error.
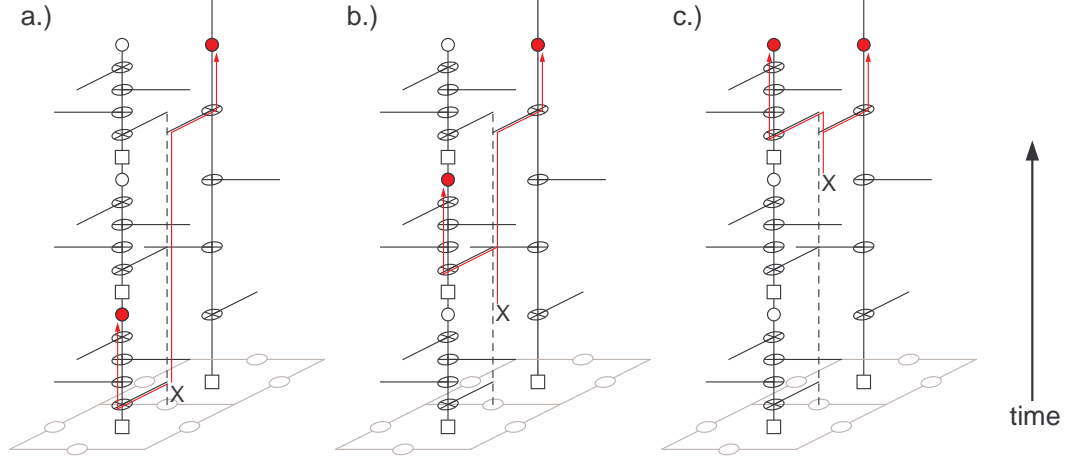
Fig. 7. Example of propagation of data errors when one syndrome is measured more frequently than another. Changed syndromes are indicated in red.

possible to say whether the gates associated with a given syndrome measurement occurred strictly before or after those associated with any other syndrome measurement.

Consider a pair of neighboring Z stabilizers sharing a single data qubit. Let us imagine that one stabilizer is measured more frequently than the other. X errors occurring on the data qubit at different times will be detected by the adjacent stabilizer measurements in a number of different ways as shown in Fig. 7. These are all single-error processes. As such, the pairs of changed syndromes indicated in red should all be connected. These connections, along with vertical connections between same site syndrome measurements and connections of the form shown in Fig. 5 will be used to determine the correct separation of a given pair of syndrome changes. The separation of a given pair of syndrome changes is defined to be the minimum number of connections in any path connecting them.

It may seem that there must be additional connections to cover the case of two-qubit interactions suffering a two-qubit error, however this is not the case. Two-qubit XX and ZZ errors are equivalent to single X or Z errors occurring before the two-qubit gate. Two-qubit errors consisting of both X and Z operators give rise to propagated errors that are handled independently by the two types of error correction.

The separation of any given pair of syndrome changes is now calculated by determining the number of edges in the shortest path connecting them. When all gates take the same time, the ideal execution order remains as shown in Fig. 2b. Nevertheless, as can be seen in Fig. 8, the new method of calculating the separation, a modification of the classical processing only, dramatically changes the performance of surface code QEC. The threshold error rate remains unchanged at approximately 0.75%. A lattice of distance d can now reliably correct $\lfloor (d-1)/2 \rfloor$ errors. For large d, the new approach provides a quadratic improvement of the logical error rate. Even for modest parameters, such as $p_g = 10^{-4}$ and $d = 7$, this translates to a logical error rate improvement of over two orders of magnitude.
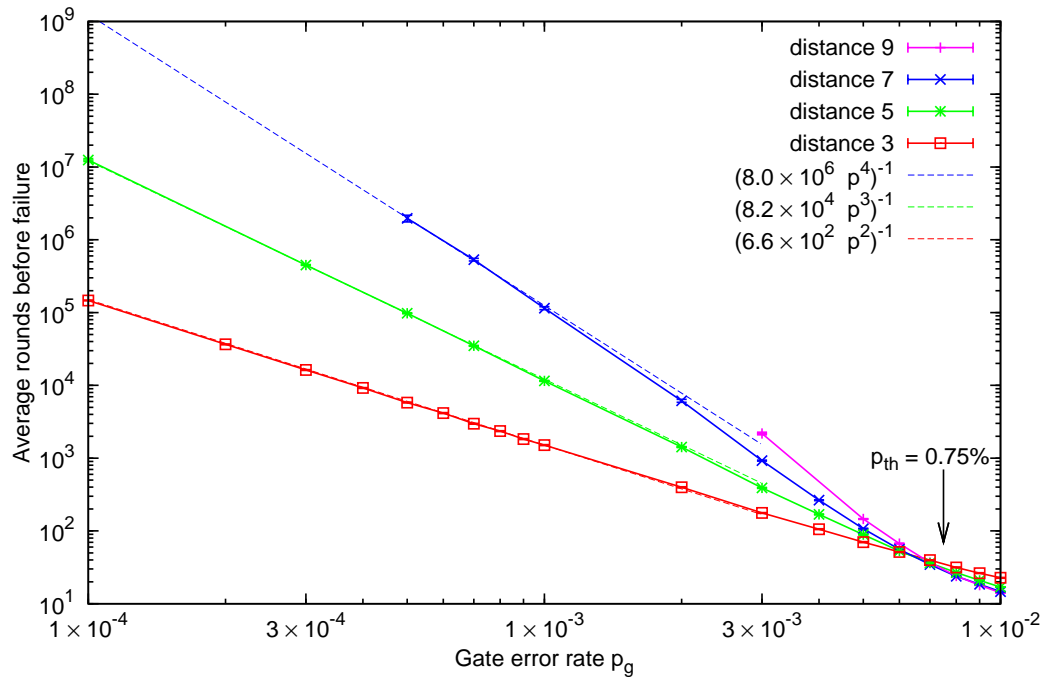
Fig. 8. Average number of rounds of error correction before the logical qubit is corrupted as a function of the physical gate error rate p_g and code distance d when the separation s of syndrome changes is calculated taking the propagation of errors by two-qubit gates into account.

5   Conclusion

By accurately tracking the propagation of errors due to the two-qubit gates use during surface code QEC, we have improved the number of errors a $d \times d$ code can reliably correct from $\lfloor (d-1)/4 \rfloor$ to $\lfloor (d-1)/2 \rfloor$, which is optimal. Explicitly, given a gate error rate $p_g = 10^{-4}$ and a surface code logical qubit with $d = 7$ (a 13×13 physical qubit lattice), our method leads to over two orders of magnitude improvement in the reliability of the logical qubit. This improvement is purely as a result of better classical processing. In the limit of large d, the new approach provides a quadratic improvement of the logical error rate.

Acknowledgements

References

1. R. P. Feynman, Int. J. Theor. Phys. **21**, 467 (1982).
2. P. W. Shor, in *Proc. 35th Annual Symposium on Foundations of Computer Science* (1994), 124–134, quant-ph/9508027.
3. P. W. Shor, Phys. Rev. A **52**, R2493 (1995).
4. E. Knill, R. Laflamme, and W. H. Zurek, Tech. Rep. LAUR-96-2199, Los Alamos National Laboratory (1996), quant-ph/9610011.
5. D. Aharonov and M. Ben-Or, Proc. ACM STOC **29**, 176 (1997), quant-ph/9611025.
6. D. Aharonov and M. Ben-Or, quant-ph/9906129 (1999).
7. E. Knill, Nature **434**, 39 (2005), quant-ph/0410199.
8. K. Fujii and K. Yamamoto, Phys. Rev. A **81**, 042324 (2010), arXiv:0912.5150.
9. A. M. Stephens and Z. W. E. Evans, Phys. Rev. A **80**, 022313 (2009), arXiv:0902.2658.
10. A. M. Stephens, A. G. Fowler, and L. C. L. Hollenberg, Quant. Info. Comp. **8**, 330 (2008), quant-ph/0702201.
11. A. G. Fowler, W. F. Thompson, Z. Yan, A. M. Stephens, B. L. T. Plourde, and F. K. Wilhelm, Phys. Rev. B **76**, 174507 (2007), cond-mat/0702620.
12. F. Helmer, M. Mariantoni, A. G. Fowler, J. von Delft, E. Solano,and F. Marquardt, Euro. Phys. Lett. **85**, 50007 (2009), arXiv:0706.3625.
13. T. Szkopek, H. Fan, V. Roychowdhury, E. Yablonovitch, P. O. Boykin, G. Simms, M. Gyure, and B. Fong, IEEE Trans. Nano. **5**, 42 (2006), quant-ph/0411111.
14. K. M. Svore, B. M. Terhal, and D. P. DiVincenzo, Phys. Rev. A **72**, 022317 (2005), quant-ph/0410047.
15. S. B. Bravyi and A. Y. Kitaev, quant-ph/9811052.
16. E. Dennis, A. Kitaev, A. Landahl, and J. Preskill, J. Math. Phys. **43**, 4452 (2002), quant-ph/0110143.
17. R. Raussendorf, J. Harrington, and K. Goyal, Ann. Phys. **321**, 2242 (2006), quant-ph/0510135.
18. R. Raussendorf and J. Harrington, Phys. Rev. Lett. **98**, 190504 (.2007), quant-ph/0610082.
19. R. Raussendorf, J. Harrington, and K. Goyal, New J. Phys. **9**, 199 (2007), quant-ph/0703143.
20. H. Bombin and M. A. Martin-Delgado, Phys. Rev. A **73**, 062303 (2006), quant-ph/0602063.
21. H. Bombin and M. A. Martin-Delgado, Phys. Rev. Lett. **97**, 180501 (2006), quant-ph/0605138.
22. H. Bombin and M. A. Martin-Delgado, Phys. Rev. Lett. **98**, 160502 (2007), quant-ph/0610024.
23. H. Bombin and M. A. Martin-Delgado, Phys. Rev. A **76**, 012305 (2007), quant-ph/0703272.
24. H. Bombin and M. A. Martin-Delgado, J. Phys. A: Math. Theor. **42**, 095302 (2009), arXiv:0704.2540.
25. H. Bombin and M. A. Martin-Delgado, Phys. Rev. A **77**, 042322 (2008), arXiv:0711.0468.

26. H. G. Katzgraber, H. Bombin, R. S. Andrist, and M. A. Martin-Delgado, Phys. Rev. A **81**, 012319 (2010), arXiv:0910.0573.
27. T. M. Stace, S. D. Barrett, and A. C. Doherty, Phys. Rev. Lett. **102**, 200501 (2009), arXiv:0904.3556.
28. T. M. Stace and S. D. Barrett, Phys. Rev. A, **81**, 022317, (2010) arXiv:0912.1159.
29. G. Duclos-Cianci and D. Poulin, Phys. Rev. Lett. **104**, 050504 (2010), arXiv:0911.0581.
30. A. G. Fowler, A. M. Stephens, and P. Groszkowski, Phys. Rev. A **80**, 052312 (2009), arXiv:0803.0272.
31. A. G. Fowler and K. Goyal, Quant. Info. Comput. **9**, 721 (2009), arXiv:0805.3202.
32. A. G. Fowler, D. S. Wang, T. D. Ladd, R. Van Meter, and L. C. L. Hollenberg, Phys. Rev. Lett. **104**, 180503 (2010), arXiv:0910.4074.
33. D. S. Wang, A. G. Fowler, A. M. Stephens, and L. C. L. Hollenberg, Quant. Info. Comp. **10**, 456 (2010), arXiv:0905.0531.
34. D. S. Wang, A. G. Fowler, C. D. Hill, and L. C. L. Hollenberg, Quant. Info. Comp. **10**, 780, (2010), arXiv:0907.1708.
35. S. J. Devitt, A. G. Fowler, T. Tilma, W. J. Munro, and K. Nemoto, International Journal of Quantum Information **8**, 1 (2010), arXiv:0906.0415.
36. L. DiCarlo, J. M. Chow, J. M. Gambetta, L. S. Bishop, B. R. Johnson, D. I. Schuster, J. Majer, A. Blais, L. Frunzio, S. M. Girvin, et al., Nature **460**, 240 (2009), arXiv:0903.2030.
37. G. Passante, O. Moussa, C. A. Ryan, and R. Laflamme, Phys. Rev. Lett. **103**, 250501 (2009), arXiv:0909.1550.
38. R. Stock and D. F. V. James, Phys. Rev. Lett. **102**, 170501 (2009), arXiv:0808.1591.
39. S. J. Devitt, A. D. Greentree, R. Ionicioiu, J. L. O'Brien, W. J. Munro, and L. C. L. Hollenberg, Phys. Rev. A **76**, 052312 (2007), arXiv:0706.2226.
40. A. M. Stephens, Z. W. E. Evans, S. J. Devitt, A. D. Greentree, A. G. Fowler, W. J. Munro, J. L. O'Brien, K. Nemoto, and L. C. L. Hollenberg, Phys. Rev. A **78**, 032318 (2008), arXiv:0805.3592.
41. S. J. Devitt, A. G. Fowler, A. M. Stephens, A. D. Greentree, L. C. L. Hollenberg, W. J. Munro, and K. Nemoto, New. J. Phys. **11**, 083032 (2009), arXiv:0808.1782.
42. R. Van Meter, T. D. Ladd, A. G. Fowler, and Y. Yamamoto, Int. J. Quantum Inf. **8**, 295 (2010), arXiv:0906.2686.
43. D. P. DiVincenzo, arXiv:0905.4839 (2009), Nobel Symposium on Qubits for Quantum Information.
44. W.-B. Gao, A. G. Fowler, R. Raussendorf, X.-C. Yao, H. Lu, P. Xu, C.-Y. Lu, C.-Z. Peng, Y. Deng, Z.-B. Chen, et al., arXiv:0905.1542 (2009).
45. R. B. Blakestad, C. Ospelkaus, A. P. VanDevender, J. M. Amini, J. Britton, D. Leibfried, and D. J. Wineland, Phys. Rev. Lett. **102**, 153002 (2009), arXiv:0901.0533.
46. D. Leibrandt, J. Labaziewicz, R. Clark, I. Chuang, R. Epstein, C. Ospelkaus, J. Wesenberg, J. Bollinger, D. Leibfried, D. Wineland, et al., Quant. Info. Comp. **9**, 901 (2009), arXiv:0904.2599.
47. J. P. Home, D. Hanneke, J. D. Jost, J. M. Amini, D. Leibfried, and D. J. Wineland, Science **325**, 1227 (2009), arXiv:0907.1865.
48. D. Hanneke, J. P. Home, J. D. Jost, J. M. Amini, D. Leibfried, and D. J. Wineland, Nature Physics **6**, 13 (2009), arXiv:0908.3031.
49. J. M. Amini, H. Uys, J. H. Wesenberg, S. Seidelin, J. Britton, J. J. Bollinger, D. Leibfried, C. Ospelkaus, A. P. VanDevender, and D. J. Wineland, arXiv:0909.2464 (2009).
50. J. Fortágh and C. Zimmermann, Rev. Mod. Phys. **79**, 235 (2007).
51. M. F. Riedel, P. Bhi, Y. Li, T. W. Hänsch, A. Sinatra, and P. Treutlein, arXiv:1003.1651 (2010).
52. M. F. Bocko, A. M. Herr, and M. J. Feldman, Rev. Mod. Phys. **80**, 885 (2008).
53. C. Becker, P. Soltan-Panahi, J. Kronjäger, S. Dörscher, K. Bongs, and K. Sengstock, arXiv:0912.3646 (2009).
54. R. C. Bialczak, M. Ansmann, M. Hofheinz, E. Lucero, M. Neeley, A. O'Connell, D. Sank, H. Wang, J. Wenner, M. Steffen, A. Cleland and J. Martinis, Nature Physics, **6**, 409–413 (2010), arXiv:0910.1118.

55. J. M. Taylor, H.-A. Engel, W. Dür, A. Yacoby, C. M. Marcus, P. Zoller, and M. D. Lukin, Nature Physics **1**, 177 (2005).
56. L. C. L. Hollenberg, A. D. Greentree, A. G. Fowler, and C. J. Wellard, Phys. Rev. B **74**, 045311 (2006), quant-ph/0506198.
57. S. A. Lyon, Phys. Rev. A **74**, 052338 (2006), cond-mat/0301581.
58. J. Edmonds, Canad. J. Math. **17**, 449 (1965).
59. J. Edmonds, J. Res. Nat. Bur. Standards **69B**, 125 (1965).
60. V. Kolmogorov, Mathematical Programming Computation **1**, 43 (2009).